IEEE Access
Multidisciplinary | Rapid Review | Open Access Journal

Received February 11, 2017, accepted April 14, 2017, date of publication May 9, 2017, date of current version June 28, 2017.

Digital Object Identifier 10.1109/ACCESS.2017.2702713

On the Analog Self-Interference Cancellation for Full-Duplex Communications With Imperfect Channel State Information

DONGLIN LIU[1], YING SHEN[1], SHIHAI SHAO[1], (Member, IEEE), YOUXI TANG[1], AND YI GONG[2], (Senior Member, IEEE)

[1]National Key Laboratory of Science and Technology on Communications, University of Electronic Science and Technology of China, Chengdu 611731, China
[2]Department of Electrical and Electronic Engineering, Southern University of Science and Technology, Shenzhen 518055, China

Corresponding author: Yi Gong (gongy@sustc.edu.cn)

This work was supported in part by the National Natural Science Foundation of China under Grant 61531009 and Grant 61471108, in part by the National Major Projects under Grant 2016ZX03001009, in part by the China Scholarship Council under Grant 201706070084, in part by the Guangdong Science and Technology Program under Grant 2016A010101003, in part by the Shenzhen Science and Technology Program under Grant KQJSCX20160226193545, and in part by the Fundamental Research Funds for the Central Universities.

ABSTRACT This paper studies the performance of the analog multi-tap (MT) canceller, where the tap coefficients are calculated based on the estimated self-interference (SI) channel state information (CSI). In this paper, both the time-invariant and the time-varying SI channels scenarios are investigated, considering the dynamic range of the analog-to-digital converter (ADC) and the linearity of the receiver chain. Closed-form expressions are first developed to calculate the residual SI power after the MT cancellation, characterizing the joint effects of the imperfect SI CSI, reconstruction errors on the estimated SI CSI, and the variation of the SI channels. Then, the achievable rate of the full-duplex transceivers is derived as a function of the residual SI power after the MT cancellation, dynamic range of the ADC, and the linearity of the receiver chain. Theoretical and simulated results show that with imperfect SI CSI, deploying more taps may harm the amount of analog SI cancellation. The sensitivity of the canceller to the doppler frequency shift reduces the amount of analog SI cancellation, and thus brings rate gain loss even with a doppler negligible in conventional communications.

INDEX TERMS Full duplex, self-interference cancellation, time-varying channels, channel state information.

I. INTRODUCTION

The ever-increasing demand for the high speed transmissions of mobile data has pushed the evolutions of wireless communication systems toward higher spectrum and energy efficiencies with lower end-to-end latency [1]–[3]. Among various technologies, full-duplex (FD) has recently attracted extensive attentions in both the academia and industry for its benefits of potentially doubling the spectral efficiency [3], [4], reducing the feedback delay [5], [6], and improving the network secrecy [7], [8]. Efficient self-interference (SI) cancellation at the FD radios is the key to realize these aforementioned advantages.

In general, a typical three-stage cancellation technique, including the propagation-domain, analog-circuit-domain, and digital-domain cancellation, is adopted for SI cancellation [3]. The propagation-domain SI suppression is implemented in two ways: 1) Isolate the transmit and receive chains by the separate-antenna architecture with SI reduction methods, such as absorptive shielding [9], cross-polarization [10], antenna directionality [11], and beam-forming [12]; and 2) share the antenna for transmission and receiving with a circulator [13], directional couplers [14], or hybrid transformers [15]. The analog-circuit-domain and digital-domain cancellation respectively reconstruct the SI signal and subtract it from the received signal based on the estimated SI channel state information (CSI) [13], [16], [17] or self-adaptive algorithms [18], [20]–[22].

The popular analog-circuit-domain SI (ASI) cancellation is usually deployed at the input of the receiver chain. For cancelling wide-band SI signals, the channel-aware multi-tap (MT) ASI canceller [13], [18], [20] is preferred, which takes into account both the direct- and reflected-path components of SI. A typical MT-ASI canceller is designed in a tapped-delay-line (TDL) architecture with a tap-dependent

transmission line for delaying the input signal, a variable attenuator, and a variable phase shifter on each tap. The MT-ASI canceller can be controlled according to the estimated SI CSI [13], [23]: 1) During the initial stage, only SI with a relatively small power is transmitted to estimate the SI CSI, based on which, the tap coefficients of the canceller are calculated. Then, 2) FD transmission is carried out with the variable attenuator and the variable phase shifter on each tap tuned according to the calculated tap coefficients. Another alternative tuning method for the canceller is to adopt the adaptive filter algorithms [18], [20]. Both the two tuning methods exhibited effective SI reduction in previous experimental trials [13], [18], [21].

In general, for ASI cancellation, adopting sophisticated filtering techniques is unaffordable due to the complexity of implementing such algorithms in analog circuit domain [3]. As a result, the performance of the ASI cancellation is more susceptible to the *tap delay alignment error*, i.e., the error between the corresponding tap delay of the canceller and that of the SI channel, imperfect SI CSI, and the variation of the SI channels, etc. However, the ASI cancellation is of essential importance for FD receivers which only have limited dynamic range of the ADC and linearity in the receiver chain. The ASI cancellation should provide an adequate amount of SI cancellation, or the residual SI after cancellation would result in significant nonlinearities at the receiver chain and raise the power of the quantization noise induced by the ADC. Thus, even if the transmitted SI could be perfectly cancelled after the digital-domain cancellation, the resultant nonlinearities and quantization noise would remain in the received signal and harm the signal-to-interference-plus-noise ratio (SINR) of the intended signal [3]. Examples in [3], [13], and [24] regarding the required amount of ASI cancellation had been explained concisely in link budget in order to achieve a SINR equal to that of a half-duplex counterpart.

Despite the research advances in ASI cancellation, current literature mainly presents simulation- and experiment-based results regarding the MT-ASI cancellation [13], [18], [20], [21], [28]. Theoretical analysis and insight is missing from the current literature about the MT-ASI canceller:

No theoretical expressions are developed to characterize the performance of the MT-ASI cancellation scheme. The effect of reconstruction errors on the achievable amount of ASI cancellation is not clear. Reconstruction errors may result from the tap delay alignment error, imperfect SI CSI, and the variation of the SI channels, etc. The lack of analytical results and insight leads to a dilemma in determining what achievable gain to be expected from FD radios. For example, deploying FD-capable mobile devices has recently attracted new attentions to fully capitalize on the benefits of FD radios [28], [29]. In this scenario, the time-varying SI channel becomes another prominent challenge for ASI cancellation in experimental trials to support FD-capable mobile devices. However, the effect of time-varying SI channels on ASI cancellation and on the achievable rate of FD communications is unclear.

Motivated by the above issues, this paper studies the performance of the MT-ASI cancellation scheme, considering the residual SI power for both the cases of the time-invariant and time-varying SI channels. Then, the achievable SINR, which is closely related to the residual power after ASI cancellation, is obtained for FD receivers with limited dynamic range of the ADC and linearity in the receiver chain. The achievable rate gain over half-duplex (HD) communications is presented in time-invariant and time-varying SI channels. The contributions are summarized as follows.

1) Closed-form expressions are developed to calculated the residual SI power after the MT cancellation, which characterize the joint effect of the imperfect SI CSI and reconstruction errors on the SI CSI. Three cases to minimize/reduce the power of the residual SI are discussed over the time-invariant SI channels. Then the results are extended to the time-varying SI channels. It is demonstrated that the optimal number of taps for the canceller, which minimizes the residual SI power, should be the least number of taps that covers the bandwidth of the received SI. Deploying more taps will enlarge the effect of the imperfect CSI, and thus, harm the ASI cancellation. In addition, the tap delay alignment of the canceller is shown to be the critical issue for the canceller. A delay alignment error larger than 1% implies that the reconstruction error dominated the performance of the canceller. In this case, increasing the accuracy of the SI channel contributes little to the cancellation.
2) The achievable rate gain over HD transceivers is discussed conditioned on imperfect SI CSI, imperfect reconstruction of the estimated CSI, as well as the time-varying SI channels for FD receivers with limited linearity and ADC dynamic range. In order to maintain the rate gain over HD transceivers, the residual SI power after ASI cancellation should be upper-bounded. However, this bound is reduced in time-varying SI channels, implying the maximum allowed transmit power (MATP) of the SI should also be reduced. The sensitivity of the channel-aware ASI canceller to the doppler frequency shift limits the amount of ASI cancellation, and thus leads to rate gain loss or lower MATP for FD receivers with limited dynamic range of the ADC and linearity in the receiver chain.

The remainder of this paper is organized as follows. In Section II, the system model is presented. Then, the residual SI power after ASI cancellation is derived over time-invariant and -variant SI channels in Section III. Next, the achievable rate gain over HD transceivers are demonstrated. Lastly, conclusions are drawn in Section V.

II. SYSTEM MODEL

In this section, the structure of a multi-tap analog SI canceller, which enables effective ASI cancellation in

FD radios [3], [13], [18], [23], is first reviewed, as well as the method to calculate the tap coefficients of this canceller. Then, the resultant SINR for FD transceivers is derived, considering the dynamic range of the ADC and the linearity of the receiver chain.

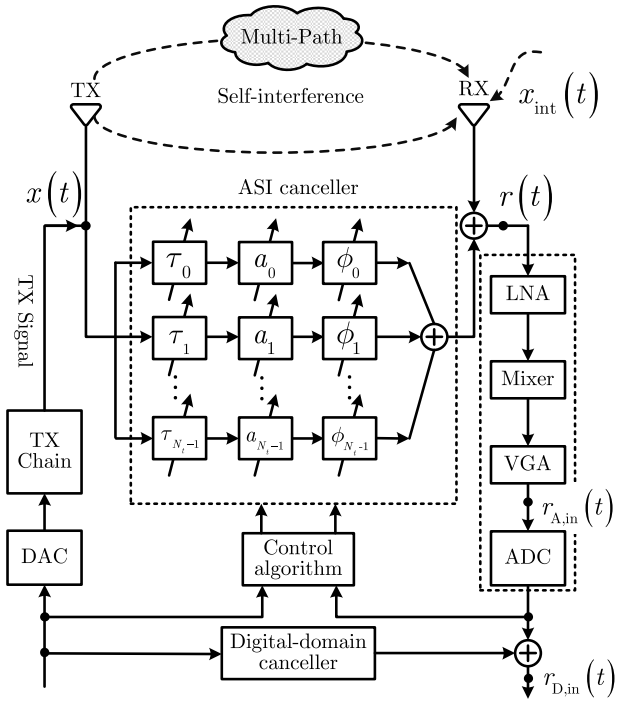

FIGURE 1. Diagram of a FD transceiver with a general MT canceller, where τ_n denotes the tap delay, a_n denotes the variable attenuator, ϕ_n denotes the phase shifter, and N_t is the number of the taps.

A. MULTI-TAP ANALOG SI CANCELLATION

Fig. 1 depicts a general TDL-based MT canceller with one transmit and one receive antennas. In this paper, the canceller is tuned according to the estimated SI CSI [13], [23]: 1) During the initial stage, only SI with a small power is transmitted to estimate the SI CSI. Based on the estimated CSI, the tap coefficients of the canceller are calculated. Then, 2) FD transmission is carried out with the canceller deployed for SI reduction. The input signal of the canceller is coupled with the transmit antenna feed. As the nth ($0 \le n \le N_t - 1$) signaling tap shown in Fig. 1, the coupled signal first goes through a path-dependent transmission line with delay τ_n ($\tau_n \ge 0$). Then its amplitude and phase are adjusted according to the calculated tap coefficients by a variable attenuator a_n and a variable phase shifter ϕ_n individually. Finally, combine the N_t paths' outputs and generate the output of the considered MT canceller for SI reduction. The received signal after the ASI suppression is given as

$$r(t) = x(t) * [h_{SI}(t) - h_{\text{c}}(t)] + x_{int}(t) + n(t), \quad (1)$$

where $x(t)$ denotes the transmitted SI signal, $h_{SI}(t)$ denotes the SI channel, $h_{\text{c}}(t)$ is the impulse response of the canceller, $x_{int}(t)$ is the received signal from the intended terminal, and $n(t)$ is the additive white Gaussian noise.

In this paper, the SI channel is described by a uniformly-spaced TDL model [33], [34], i.e.,

$$h_{SI}^{b}(t) = \sum_{i=0}^{\infty} h_i \delta\left(t - \frac{i}{B}\right), \quad (2)$$

where $h_{SI}^{b}(t)$ is the complex baseband equivalent form of $h_{SI}(t)$, h_i denotes the tap gain of the SI channel, B is the bandwidth of the SI signal, and $\delta(t)$ is the impulse function.

The impulse response of the canceller can be modeled as the summation of the N_t paths' responses [18], i.e.,

$$h_{\text{c}}(t) = \sum_{n=0}^{N_t-1} a_n \delta(t - \tau_n) \otimes h_{\phi_n}(t), \quad (3)$$

where $\otimes$ denotes the convolution operation, $h_{\phi_n}(t)$ is the impulse response of the nth phase shifter and can be modeled as an all-pass filter with

$$h_{\phi_n}(t) = \cos(\phi_n)\delta(t) + \sin(\phi_n)\frac{1}{\pi t}. \quad (4)$$

By combining (3) and (4) and performing the Fourier transformation, the frequency response of the canceller is given by [18]

$$H_c(j\omega) = \begin{cases} \sum_{n=0}^{N_t-1} a_n e^{-j\phi_n} e^{-j\omega\tau_n}, \omega \ge 0 \\ \sum_{n=0}^{N_t-1} a_n e^{j\phi_n} e^{-j\omega\tau_n}, \omega < 0, \end{cases} \quad (5)$$

with ω representing the angular frequency. Formula (5) captures the key parameters of each tap more conveniently in the frequency domain, and will be adopted in rest of the paper. With a sampling interval of $\Delta_w = 2\pi B/K$, the sampled versions of (5) can be written as [23]

$$H_c(k) = H_c(j\Delta_w k) = \Psi_k^T W, \quad (6)$$

where K is the total number of samples, $\Psi_k = \left[e^{-j\Delta_w k\tau_1}, \cdots, e^{-j\Delta_w k\tau_{N_t}}\right]^T$, $W = \left[a_1 e^{j\phi_1}, \cdots, a_{N_t} e^{j\phi_{N_t}}\right]^T$, and $(\cdot)^T$ represents the transposition of a vector or matrix. Since Ψ_k is determined by time delays $\{\tau_n\}$, Ψ_k is a constant with fixed τ_n.

In what follows, the method to calculate the tap coefficients of this canceller according to the estimated SI CSI is given in details.

1) IMPERFECT SI CHANNEL ESTIMATION

In this paper, channel-aware ASI cancellation technique is adopted [3], [13]: Based on the estimated SI channel, the parameters $\{a_n\}$ $\{\phi_n\}$ are determined for the canceller according to the minimum mean-squared error criteria.

In the sequel, the orthogonal frequency division multiplexing (OFDM) modulation is adopted, and pilot-aided channel estimation with the LS estimator [35] is utilized to obtain the

CSI of the SI channel.[1] Consider an OFDM system with K subcarriers and K_G points of the cyclic prefix. Supposing that the duration of one OFDM symbol is T, the received signal is then sampled at rate $1/T_s$, where $T_s = T/(K + K_G)$. For the case that the SI channel is quasi-static over one OFDM symbol duration, the received signal at the kth subcarrier is given as

$$R(k) = H(k) X(k) + N(k), \tag{7}$$

where $X(k)$ is the transmitted signal at the kth subcarrier, treated as known information, $N(k)$ is the circularly symmetric complex Gaussian (CSCG) noise with zero mean and variance σ^2, and $H(k)$ is the frequency-domain SI channel expressed as [38]

$$H(k) = \sum_{l=0}^{L_f-1} h_l e^{-j2\pi kl/K}, \tag{8}$$

with h_l representing the l-th tap gain of the SI channel shown in (2) and L_f representing the length of the SI channel response identified by the channel estimator.

It is noted that the whole OFDM symbol can be treated as known pilots to estimate the SI channel, since the receiver has perfect knowledge of the transmitted symbols. As such, utilizing the LS estimator, the estimated channel response is obtained as [35], [38]

$$\begin{aligned}\hat{H}(k) &= \frac{R(k) X^*(k)}{|X(k)|^2} \\ &= H(k) + \bar{N}(k),\end{aligned} \tag{9}$$

where $|\cdot|$ denotes 2-norm of a vector, $(\cdot)^*$ denotes the conjugate operation, and $\bar{N}(k)$ is the equivalent CSCG noise with zero mean and variance $\tilde{\sigma}^2$.

2) RECONSTRUCTION OF THE SI CHANNEL RESPONSES

Adopting the estimated SI channel, the tap coefficients are then calculated. For given $\{\tau_n\}, n = 0, 1, \cdots, N_t - 1$, McMichael's method [23] can be utilized to compute the optimum parameters $\{a_n\}$ and $\{\phi_n\}$ to match the SI channel.

[1] In the estimation process, the non-ideal components of the SI, such as the non-linearities produced by the power amplifier and phase noise, is simply treated as Gaussian noise [36], [37].

The key idea in [23] is to minimize the mean-square error of the reconstructed SI channel response. Denote $\hat{H} = \left\{\hat{H}(0), \cdots, \hat{H}(K-1)\right\}^T$. For given $\{\tau_n\}$, the optimal tap coefficients of the canceller for imitating $\hat{H}$ is a Wiener solution [23], [39]

$$W_0 = R^{-1} P, \tag{10}$$

where R is given in (11), as shown at the bottom of this page, and P is a complex cross-correlation matrix defined as

$$P = \frac{1}{K} \sum_{k=0}^{K-1} \hat{H}(k) \Psi_k^*. \tag{12}$$

Therefore, based on the imperfect SI CSI, the reconstructed frequency response of the MT canceller is given as $H_c = \left\{\Psi_0^T W_0, \cdots, \Psi_{K-1}^T W_0\right\}^T$. Denote the SI channel as a vector form $H = \{H(0), \cdots, H(K-1)\}^T$ and the SI signal by $X = diag\{X(0), \cdots, X(K-1)\}$. The power of the residual SI is represented by the average subcarrier-wise power of the SI signal after the ASI cancellation [27] and can be computed as

$$p_{rd} = \frac{1}{K} \mathbb{E}\left\{|X(H - H_c)|^2\right\}, \tag{13}$$

which will be given in closed-form expressions in the next section.

B. ACHIEVABLE SINR OF FD TRANSCEIVERS

This paper considers a FD direct-conversion transceiver model [24] shown in Fig. 1. After the ASI cancellation and following the signal processing along the receiver chain, $r(t)$ first passes through a low-noise amplifier (LNA) and is down-converted by the mixer. After the lowpass filtering and gain adjustment by the VGA, the signal at the interface of the ADC input can be approximately written as [24]

$$\begin{aligned}r_{A,in}(t) = &\sqrt{g_{rx}} r_{rd}^b(t) + \sqrt{g_{rx}} x_{int}^b(t) \\ &+ x_2(t) + x_3(t) + n_{A,in}(t),\end{aligned} \tag{14}$$

where $\sqrt{g_{rx}}$ denotes the total gain of the RF chain, $r_{rd}^b(t) = LPF\left\{\{x(t) \otimes [h_{SI}(t) - h_c(t)]\} e^{-jw_c t}\right\}$ is the complex baseband form of the downconverted residual SI signal after ASI cancellation with w_c being the carrier frequency and

$$R = \frac{1}{K}\Re = \frac{1}{K}\begin{bmatrix} K & \sum_{k=0}^{K-1} e^{j\Delta_w k(\tau_0-\tau_1)} & \cdots & \sum_{k=0}^{K-1} e^{j\Delta_w k(\tau_0-\tau_{N_t-1})} \\ \sum_{k=0}^{K-1} e^{j\Delta_w k(\tau_1-\tau_0)} & K & \cdots & \sum_{k=0}^{K-1} e^{j\Delta_w k(\tau_1-\tau_{N_t-1})} \\ \vdots & \vdots & \ddots & \vdots \\ \sum_{k=0}^{K-1} e^{j\Delta_w k(\tau_{N_t-1}-\tau_0)} & \sum_{k=0}^{K-1} e^{j\Delta_w k(\tau_{N_t-1}-\tau_1)} & \cdots & K \end{bmatrix} \tag{11}$$

LPF denoting the lowpass filtering, $x_{int}^{b}(t)$ is the complex baseband form of the downconverted intended signal, $x_2(t)$ and $x_3(t)$ are respectively the 2nd- and 3rd-order nonlinear distortion produced at the RX chain, and $n_{A,in}(t)$ denotes the accumulated CSCG noise before the ADC.

After sampling $r_{A,in}(t)$ by the ADC and deploying digital cancellation to cancel SI [25], [27], the obtained signal can be written as

$$r_{D,in}(n) = r_{rdSI}(n) + \sqrt{g_{rx}}x_{int}^{b}(n) + x_2(n) + x_3(n) + n_{A,in}(n) + n_Q(n), \quad (15)$$

where $r_{rdSI}(n) = r_{rd}^{b}(n) - r_{c}^{b}(n)$ is the residual SI signal after the digital cancellation, with $r_{c}^{b}(n)$ being the digital-domain reconstructed SI signal, and $n_Q(n)$ denotes the quantization noise due to the limited dynamic range of the ADC.

In this paper, the 2nd- and 3rd-order nonlinear distortion produced in the receiver chain are respectively modeled by adopting the 2nd- and 3rd-order input referred intercept points, i.e., IIP2 and IIP3 figures [32]. The power of the 2nd- and 3rd-order nonlinear distortion can be respectively written as [24]

$$p_2 \approx g_L^2 g_M g_V p_{in}^2 \left(\frac{1}{ip2_M} + \frac{g_M}{ip2_V}\right) \quad (16)$$

and

$$p_3 \approx g_L g_M g_V p_{in}^3 \times \left[\left(\frac{1}{ip3_L}\right)^2 + \left(\frac{g_L}{ip3_M}\right)^2 + \left(\frac{g_L g_M}{ip3_V}\right)^2\right], \quad (17)$$

where g_L, g_M, and g_V respectively denote the gain of the components of LNA, Mixer, and VGA, $ip2_L$, $ip2_M$, and $ip2_V$ respectively denote the 2nd-order input intercept point of LNA, Mixer, and VGA, $ip3_L$, $ip3_M$, and $ip3_V$ respectively denote the 3rd-order input intercept point of LNA, Mixer, and VGA, and $p_{in} \approx p_{rd}$ since the residual SI signal after ASI cancellation is generally the dominant signal component.

Following the well-established theory on ADCs [32], the power of the quantization noise induced by the ADC, i.e., $n_Q(n)$ in (15), is modeled as

$$P_{qn,dB} = P_{Target} - 6.02b - 4.76 + \rho \; dBm, \quad (18)$$

where $P_{qn,dB}$ is the quantization noise mearsured in dBm, b denotes the effective number of bits (ENOB) of the ADC, P_{Target} denotes the maximum allowed average power of the signal at the ADC input and ρ is the peak-to-average power ratio. P_{Target} in (18) is an ADC-dependent constant. By using P_{Target}, g_{rx} can be approximated as [24]

$$g_{rx} \approx \frac{p_{Target}}{p_{rd}}, \quad (19)$$

where $p_{Target} = 10^{P_{Target}/10-3}$.

Therefore, the achievable SINR for the intended signal after the digital-domain cancellation can be written as [24]

$$\beta_{D,in} = \frac{g_{rx}p_{int}}{g_{rx}\sigma_{in}^2 + p_{rdSI} + p_2 + p_3 + p_Q} = \frac{\beta_{hf}}{1 + \frac{p_{rdSI}+p_2+p_3+p_Q}{g_{rx}\sigma_{in}^2}}, \quad (20)$$

where p_2, p_3, p_Q, and g_{rx} are given respectively in (16)–(19) with $P_{qn,dB} = 10log_{10}(p_Q \times 1000)$, p_{int} denotes the power of the intended signal, σ_{in}^2 denotes the power of the CSCG noise, i.e., $n_{A,in}(n)$, $\beta_{hf} = p_{int}/\sigma_{in}^2$ denotes the signal-to-noise ratio (SNR) achievable in HD communications, and p_{rdSI} denotes the power of residual SI after the digital-domain cancellation.

It is noted that recent efforts in SI cancellation have kept p_{rdSI} negligible around the noise floor [13], [28]. Thus, p_{rdSI} is omitted in this paper and the effects of the nonlinear distortions and quantization noise in the receiver chain resulting from the residual SI after ASI cancellation are focused on. Therefore, substituting (18) and (19) into (20) yields

$$\beta_{D,in} = \frac{\beta_{hf}}{\underbrace{1 + \frac{p_{rd}(p_2+p_3)}{p_{Target}\sigma_{in}^2} + \frac{p_{rd}q_{adc}}{\sigma_{in}^2}}_{\beta_{INR}}}, \quad (21)$$

where $q_{adc} = 10^{\frac{\rho-6.02b-4.76}{10}}$. As shown in (16), (17), and (21), β_{INR}, which characterizes the powers of the nonlinear distortions and quantization noise, is the function of p_{rd}. In the next section, p_{rd} is derived in closed-form expressions for both the time-invariant and time-varying SI channels scenarios.

III. ANALYSIS ON RESIDUAL SI POWER AFTER ASI CANCELLATION

In this section, the subcarrier-wise power of the residual SI after ASI cancellation is calculated. The joint effect of estimation errors and reconstruction errors on the residual SI power is first analyzed and the design criterias for the MT canceller are discussed over the time-invariant SI channels. Then the results are extended to the time-variant SI channels.

A. RESIDUAL SI POWER OVER TIME-INVARIANT CHANNELS

1) JOINT EFFECT OF ESTIMATION AND RECONSTRUCTION ERRORS

The SI channel is considered time-invariant within a frame or longer period as in [31] and [40]. Then, the performance of the canceller is affected by error $E_c = H - H_c$. Denote the correlation matrix of E_c by

$$C_{W-S} = \mathbb{E}\left[(H - H_c)(H - H_c)^H\right]. \quad (22)$$

The power of the residual SI is represented by the average power of the SI signal after ASI cancellation, i.e.,

$$\begin{aligned} p_{rd} &= \frac{1}{K}\mathbb{E}\left\{|X(H-H_c)|^2\right\} \\ &= \frac{1}{K}\mathbb{E}\left\{tr\left[(H-H_c)(H-H_c)^H X^H X\right]\right\} \\ &= \frac{1}{K} tr\left\{C_{W-S}\right\}, \end{aligned} \tag{23}$$

where $\mathbb{E}\left[|X(k)|^2\right] = 1$ with $\mathbb{E}\left[X(k_1)X^*(k_2)\right] = 0$, $k_1 \neq k_2$, and $tr(\cdot)$ denotes the trace of a matrix. The following proposition about C_{W-S} is firstly presented to calculate p_{rd}.

Proposition 1: For the given SI channel H, the correlation matrix of E_c is given as

$$\begin{aligned} C_{W-S} = {} & \tilde{\sigma}^2\Omega\Re^{-1}\Omega^H + HH^H - \Omega\Re^{-1}\Omega^H HH^H \\ & + \Omega\Re^{-1}\Omega^H HH^H\Omega\Re^{-1}\Omega^H - HH^H\Omega\Re^{-1}\Omega^H. \end{aligned} \tag{24}$$

Proof: Denote $\Omega = \left[\Psi_1^T, \Psi_2^T, \cdots, \Psi_K^T\right]^T$, and formula (12) can be rewritten as

$$P = \frac{1}{K}\Omega^H\hat{H}. \tag{25}$$

The reconstructed frequency response of the MT canceller can be written as a vector form

$$H_c = \Omega\Re^{-1}\Omega^H\hat{H}. \tag{26}$$

Substitute (9), (6), (25), and (26) into (22), and it yields the result given in (24). ∎

Remark 1: Formula (24) depicts the joint effect of estimation and reconstruction errors that affects the performance of the canceller. The first term in (24), i.e., $\tilde{\sigma}^2\Omega\Re^{-1}\Omega^H$, is the composition error which results from the imperfect SI CSI $\hat{H}$ and the reconstruction process for reproducing $\hat{H}$. The other terms, named as reconstruction errors, are the by-products for imitating H. Proposition 1 shows that both the two types of errors are affected by the design matrix of the MT canceller, i.e., $\Omega\Re^{-1}\Omega^H$.

According to proposition 1, the power of the residual SI given in (23) is then obtained as follows.

Proposition 2: The residual SI power given in (23) is written as

$$p_{rd} = \frac{N_t}{K}\tilde{\sigma}^2 + \frac{1}{K}tr\left(HH^H - \Omega\Re^{-1}\Omega^H HH^H\right). \tag{27}$$

Proof: Calculate $\Omega^H\Omega$, and it yields

$$\Omega^H\Omega = \Re. \tag{28}$$

From (28), it follows

$$\frac{1}{K}tr\left(\tilde{\sigma}^2\Omega\Re^{-1}\Omega^H\right) = \frac{N_t}{K}\tilde{\sigma}^2 \tag{29}$$

and

$$\begin{aligned} & tr\left(\Omega\Re^{-1}\Omega^H HH^H\Omega\Re^{-1}\Omega^H - HH^H\Omega\Re^{-1}\Omega^H\right) \\ [-3pt] &= tr\left(HH^H\Omega\Re^{-1}\Omega^H\Omega\Re^{-1}\Omega^H - HH^H\Omega\Re^{-1}\Omega^H\right) \\ &= 0. \end{aligned} \tag{30}$$

Thus, by substituting (29), (30), and (24) into (23), the residual SI power given in (23) can be simplified as (27). ∎

Remark 2: In (27), the first term, i.e., $\frac{N_t}{K}\tilde{\sigma}^2$ depicts the residual SI power resulting from the composition error discussed in Remark 1. It increases linearly with the number of the taps regardless of the design matrix $\Omega\Re^{-1}\Omega^H$. Whereas the second term which denotes the residual SI power caused by the reconstruction errors in Remark 1 is affected intensely by $\Omega\Re^{-1}\Omega^H$. According to (27), $\Omega\Re^{-1}\Omega^H$ should be designed for removing or minimizing the reconstruction errors with the least number of taps N_t.

2) MINIMIZING THE RESIDUAL SI POWER

As discussed in [13] and [23], achieving a general solution for $\underset{\{a_n\},\{\phi_n\},\{\tau_n\},N_t}{minimize}\ p_{rd}$ is quite demanding. In this paper, with (27), three cases are discussed about the residual SI power. Case 1 considers the canceller holds perfect CSI of the SI channel and that the tap delays $\{\tau_n\}$ of the MT canceller are consistent with those of the SI channel, i.e., $\tau_i - \frac{i}{B} = 0$. In case 2, the residual SI power is discussed conditioned on imperfect SI CSI and perfect delay alignment as case 1. In case 3, imperfect delay alignment is considered. It is demonstrated the effect of the delay alignment error i.e., $\tau_i - \frac{i}{B} \neq 0$, can be completely removed at the cost of increasing N_t.

Case 1: Perfect CSI for SI Channel and Perfect Delay Alignment

In this case, the tap delays $\{\tau_n\}$ of the MT canceller are consistent with those of the SI channel, and the canceller holds perfect SI CSI. It is intuitive that the optimal tuning W_{op} contains

$$W_{op} = \{h_0, h_1, \ldots, h_{L_f-1}, 0, 0, \ldots\}^T, \tag{31}$$

and that the SI propagating through H is completely removed, implying its residual power $p_{rd} = 0$.

Remark 3: It is noted that $\Re$ approaches matrix KI_{N_t} [23] and the calculation of W_0 given in (10) reduces to the inverse fourier transform of H, bringing in $W_0 = 1/K\Omega^H H = W_{op}$. Thus, tuning $\{a_n\}$ and $\{\phi_n\}$ according to W_0 leads to $p_{rd} = 0$, which means the effect of the reconstruction errors discussed in Remark 1 and 2 is removed in this case, i.e.,

$$\frac{1}{K}tr\left(HH^H - \Omega\Re^{-1}\Omega^H HH^H\right) = 0. \tag{32}$$

In case 1, the optimal number of taps is $N_t \geq L_f$ with taps coefficients given in (31) or (10).

Case 2: Imperfect SI CSI while Perfect Delay Alignment

In this case, the tap delays $\{\tau_n\}$ of the MT canceller are consistent with those of the SI channel. However, the canceller holds imperfect SI CSI shown in (9). From Remark 3, with imperfect SI CSI but perfect delay alignment, formula (32) still holds since the estimation errors exert no effect on the second term in (27). Thus, the residual SI power shown in (27) only contains the power resulting from the composition error and can be reduced to

$$p_{rd} = \frac{N_t}{K}\tilde{\sigma}^2. \tag{33}$$

Remark 4: As discussed in [4], it is required that the maximum and minimum delays of the canceller should cover the delay spread of the SI channel. That is, $N_t \geq L_f$ is required for imitating H accurately. Thus, in this case, the SI power given in (27) is minimized as (33) with $N_t = L_f$. Additionally, case 2 with $N_t = L_f$ demonstrates the global optimal design for the canceller since case 2 with $N_t = L_f$ simultaneously minimizes $tr\left(HH^H - \Omega\Re^{-1}\Omega^H HH^H\right)$ as well as $\frac{N_t}{K}\tilde{\sigma}^2$.

Remark 5: The SI CSI is obtained via the LS estimator. As discussed in Remark 3, with perfect delay alignment, the canceller is in fact carrying out the inverse discrete Fourier Transform (DFT) on the estimated SI CSI. Comparing the analysis in Section III.A and (38)–(40) of [38], the whole procedure for reconstructing the SI channel response is equivalent to the Maximum Likelihood (ML) estimator given in [38]. Thus, the accuracy for reconstructing the SI channel of the MT canceller is superior to a single LS estimator.

As the delay alignment becomes non-ideal, the orthogonality of between entries of Ω^H and H is destroyed. The MT canceller suffers from the reconstruction error indicated by $\frac{1}{K}tr\left(HH^H - \Omega\Re^{-1}\Omega^H HH^H\right)$.

For small delay alignment errors, the residual SI power can be calculated via (33). The tolerance for the alignment errors will be discussed in numeral results in this section.

Case 3: Imperfect SI CSI and Imperfect Delay Alignment

In this case, the canceller only holds imperfect SI channel CSI and the tap delays of the canceller are not aligned with the ones of the SI channel, i.e, $\tau_i - \frac{i}{B} \neq 0$.

As in [13] and [23], a general solution that minimizes p_{rd} in this case is infeasible. It is noted that conditioned on large alignment errors, $\frac{1}{K}tr\left(HH^H - \Omega\Re^{-1}\Omega^H HH^H\right)$ resulting from the reconstruction errors may dominate the residual SI power. In this case, it is demonstrated that using the following proposition, $\frac{1}{K}tr\left(HH^H - \Omega\Re^{-1}\Omega^H HH^H\right) = 0$ is achievable without considering the delay alignment errors.

Proposition 3: The design matrix $\Omega\Re^{-1}\Omega^H$ of the MT canceller can be converted to an identity matrix with uniformly-spaced tap interval

$$\Delta t = \tau_{i+1} - \tau_i = 1/B \tag{34}$$

and number of taps

$$N_t = K. \tag{35}$$

Proof: See Appendix. ■

Therefore, $\frac{1}{K}tr\left(HH^H - \Omega\Re^{-1}\Omega^H HH^H\right) = 0$ holds if (34) and (35) are satisfied. The residual SI power becomes $p_{\mathrm{rd}} = \tilde{\sigma}^2$.

Remark 6: $N_t = K$ consists with the *critically fitted model* for Wiener filtering, which is a preferred design strategy to match the number of taps of Wiener filters to the order of the regression model [39]. In fact, the results in (34) and (35) can be treated as the application of sampling theorem regardless of the offset between each corresponding tap delay.

For large delay alignment errors due to practical engineering implementation, the residual SI power is determined by the reconstruction errors. Formulas (34) and (35) provide a method for completely removing the reconstruction errors at the cost of enlarging the effect of the imperfect CSI.

For wide-bandwidth SI, the sampled versions of the SI channel should increase for enhanced suppression of SI. However, the number of taps can not be increased due to varieties of reasons such as space limitations, insert loss and complexity [13], [18]. Thus, the design indicated by (34) and (35) may only work for SI signals with a relatively-narrow bandwidth.

B. RESIDUAL SI POWER OVER TIME-VARYING CHANNELS

In previous contributions, the SI channels were usually treated as time-invariant ones. However, for analog SI cancellation, the time-variant property of the SI channel should be taken into account. It is reasoned as follows. The channel-aware analog SI cancellation requires strictly real-time tuning for tracking the SI channel. There exists a processing delay from obtaining the SI CSI to producing the expected frequency response of the MT canceller for cancellation. This delay includes the consuming time of signal processing for calculating the tap coefficients, as well as the response time (setting time) of analog devices for generating the expected tap coefficients.[2] In brief, the frequency response of the canceller generated at t_1, however, is used for imitating the SI channel at time instant t_2 ($t_2 > t_1$) due to the processing delay. The delay, i.e., $\Delta t_d = t_2 - t_1$, may bring considerable performance loss of the canceller over time-varying channels.

In this paper, modeling the characteristics of Δt_d is beyond the scope of this paper. Thus, Δt_d is treated as a variable and denoted by the multiples of T_s, i.e., $\Delta t_d = \Delta T T_u$ with ΔT being an integer and $T_u = KT_s$. The delay effect is evaluated by considering that the tap parameters of the canceller remain unchanged while the channel varies such that there is a delay Δt_d between the reconstructed SI channel and the SI channel.

Conditioned on a time-varying channel, which varies from symbol to symbol, (7) still holds [41], and the autocorrelation of the F_1th and F_2th sub-carriers at the m_1th and m_2th symbols can be written as [41]–[43]

$$E\left\{H^{(m_1)}(F_1)\left[H^{(m_2)}(F_2)\right]^*\right\} = \frac{1}{K_f+1}\left\{K_f + \frac{J_0\left[2\pi\Delta T f_d T_u\right]}{1 - j2\pi\Delta F\eta}\right\}, \tag{36}$$

where $\Delta T = m_1 - m_2$, $\Delta F = F_2 - F_1$, K_f is the Ricean K-factor, $J_0(\cdot)$ is the Bessel function of the first kind of order 0, and η represents the normalized mean delay spread measure [42], [44]. Thus, the correlation matrix can be expressed as

$$\Xi(\Delta T) = E\left[H^{(m_1)}\left(H^{(m_2)}\right)^H\right], \tag{37}$$

with the (F_1, F_2)th entry defined in (36).

[2] Although this paper focuses on the MT canceller based on the estimated CSI, the delay also exists in the MT canceller based on other algorithms, such as adaptive algorithms.

Consider the SI CSI obtained based on the m_1th symbol is used for SI suppression at the m_2th symbol with $m_1 < m_2$. Hence, following similar derivation, C_{W-S} given in (23) is modified as

$$\begin{aligned} C_{W-S} &= E\left\{\left[H^{(m_2)} - H_c^{(m_1)}\right]\left[H^{(m_2)} - H_c^{(m_1)}\right]^H\right\} \\ &= \tilde{\sigma}^2\Omega\Re^{-1}\Omega^H + \Xi(0) - \Omega\Re^{-1}\Omega^H\Xi(\Delta T) \\ &\quad + \Omega\Re^{-1}\Omega^H\Xi(0)\,\Omega\Re^{-1}\Omega^H - \Omega\Re^{-1}\Omega^H\Xi(\Delta T), \end{aligned} \tag{38}$$

where $\Xi(\Delta T) = \Xi^H(\pm\Delta T)$ is used since $J_0(\cdot)$ is an even function. From the proof of proposition 2, the residual SI power is obtained as

$$\begin{aligned} p_{rd} &= \frac{N_t}{K}\tilde{\sigma}^2 + \frac{1}{K}tr\left[\Xi(0) + \Xi(0)\,\Omega\Re^{-1}\Omega^H\right] \\ &\quad - \frac{2}{K}tr\left[\Xi(\Delta T)\,\Omega\Re^{-1}\Omega^H\right]. \end{aligned} \tag{39}$$

Remark 7: As seen in (39), the first term, i.e., $\frac{N_t}{K}\tilde{\sigma}^2$ depicts the residual SI power resulting from the composition error, which has been discussed in Remark 2. Whereas, the other terms in (39) are associated with the reconstruction errors and the time variability of the SI channel due to the delay effect. The effect of the time-varying SI channel is included in $\frac{1}{K}tr\left[\Xi(0) + \Xi(0)\,\Omega\Re^{-1}\Omega^H\right] - \frac{2}{K}tr\left[\Xi(\Delta T)\,\Omega\Re^{-1}\Omega^H\right]$ through $\Xi(\Delta T)$, which enlarges p_{rd} and will be shown in the next subsection.

Recall that as discussed in remarks 3 and 5, with perfect delay alignment, $\Omega\Re^{-1}\Omega^H$ is equivalent to performing DFT and inverve DFT. Thus, with perfect delay alignment,

$$tr\left[\Xi(\Delta T)\,\Omega\Re^{-1}\Omega^H\right] = tr\left[\Xi(\Delta T)\right]. \tag{40}$$

TABLE 1. Residual SI power for the three cases.

Cases	Descriptions	Power of Residual SI
Case 1	• Perfect SI channel CSI and perfect delay alignment; • Time-varying SI channel with processing delay ΔTT_u	$2-\frac{2}{K_f+1}\left\{K_f + J_0\left[2\pi\Delta Tf_dT_u\right]\right\}$
Case 2	• Imperfect SI channel CSI and perfect delay alignment; • Time-varying SI channel with processing delay ΔTT_u	$\frac{N_t}{K}\tilde{\sigma}^2+2-\frac{2}{K_f+1}\left\{K_f + J_0\left[2\pi\Delta Tf_dT_u\right]\right\}$
Case 3	• Imperfect SI channel CSI and imperfect delay alignment with $N_t = K$ and $\Delta t = 1/B$; • Time-varying SI channel with processing delay ΔTT_u	$\tilde{\sigma}^2+2-\frac{2}{K_f+1}\left\{K_f + J_0\left[2\pi\Delta Tf_dT_u\right]\right\}$

Utilizing (40) for cases 1 and 2, and following similar analysis in proposition 3 for case 3, the residual powers over time-variant SI channels for the three cases in Subsection A are summarized in Table 1 with the gain of the SI channel normalized to 1.

C. SIMULATION AND NUMERAL RESULTS

In all the simulation, the OFDM-based FD links with 2048 subcarriers are adopted. The subcarrier spacing is 15 kHz and the length of cyclic prefix is 144 with the sampling time $T_s = 3.3 \times 10^{-8}$s. The total subcarriers are utilized for estimation for better estimation performance. The multipath channel with power profile of 0 dB, −25 dB, −30 dB, −35 dB, −40 dB, −45 dB, −50 dB, −55 dB, −60 dB, −65 dB, −70 dB, and −75 dB for delays of 0, 1, ⋯, and 11 samples (i.e., $L_f = 12$) is considered. The power profile is modified from [27] considering the first tap is normalized to 0 dB after antenna isolation and that the other taps are the results of reflected paths.

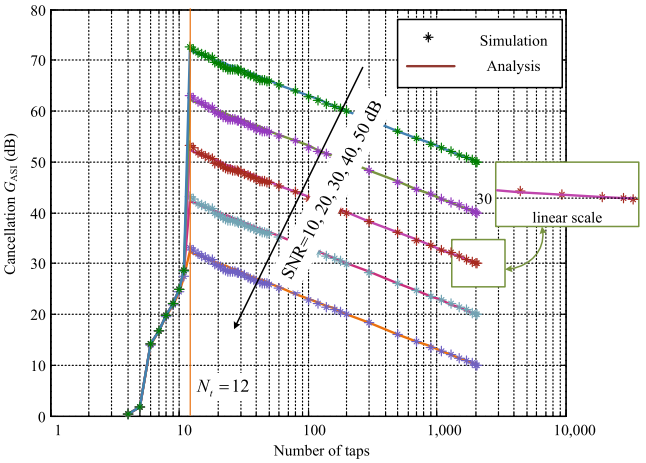

FIGURE 2. Cancellation ability versus number of taps with perfect delay alignment to the observed SI channel, where *SNR* denotes the estimator SNR for estimating the SI CSI. As a comparison, the number of taps is extended to *K*.

In this paper, the cancellation ability is evaluated by $G_{ASI} = -10\log_{10}p_{rd}$ since the power of the transmit SI is normalized to 1. Fig. 2 depicts the achievable cancellation G_{ASI} with perfect delay alignment considered in case 2. For $N_t < L_f$, especially a smaller N_t, the operational bandwidth of the canceller has not covered the SI channel adequately as discussed in [18]. Thus, the canceller provides limited cancellation. As shown in (21), in this case, the residual SI power includes the components resulting from the composition error and the reconstruction error. It is the large reconstruction error, i.e. $\frac{1}{K}tr\left(HH^H - \Omega\Re^{-1}\Omega^H HH^H\right)$ that restricts the cancellation when $N_t < L_f$. As $N_t \geq L_f$, the residual SI power resulting from the reconstruction error can be completely removed as discussed in Remark 4, and only the power of the composition error $\tilde{\sigma}^2\Omega\Re^{-1}\Omega^H$ remains, which denotes the power of the residual SI after ASI cancellation and increases linearly with N_t. Thus, a global optimum for the canceller with $N_t = L_f$ is obtained in Fig. 2.

The tolerance for the normalized delay alignment errors is also discussed. Here, the error between the corresponding tap delay of the canceller and that of the SI channel is referred to as the delay alignment error. For simplicity, these delay alignment errors are kept identical in simulations. Fig. 3 shows

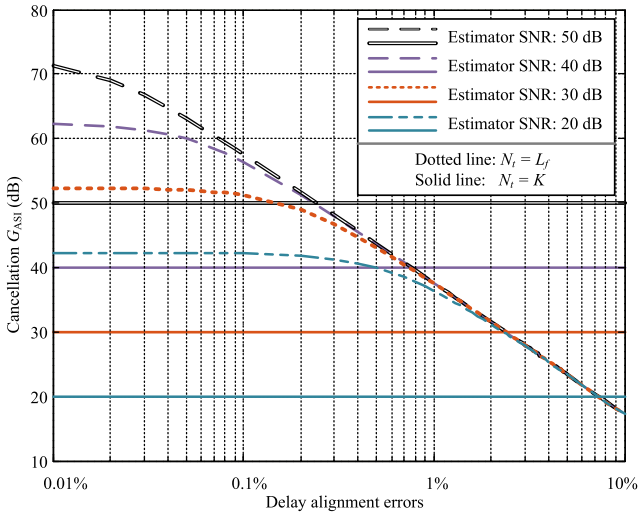

FIGURE 3. Deteriorated cancellation versus the normalized alignment errors with $N_t = L_f$ and $N_t = K$.

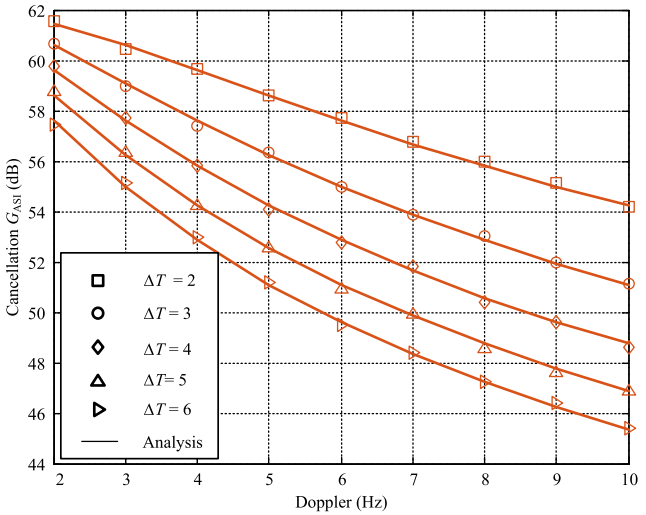

FIGURE 4. Cancellation versus Doppler with a Ricean K_f of 10 dB and an estimator SNR of 40 dB, where the markers and solid lines denote simulation and analytical results, respectively.

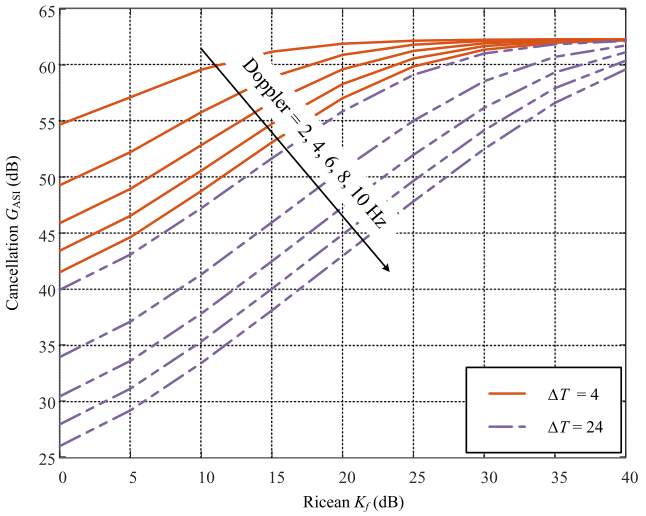

FIGURE 5. Cancellation versus Ricean K_f, where the doppler ranges from 2 Hz to 10 Hz and the estimator SNR is 40 dB.

the deteriorated cancellation versus this normalized alignment errors with $N_t = L_f$. In an estimator SNR range of 20 dB to 50 dB, which denotes the SNR for obtaining the SI CSI, a delay alignment error larger than 1% implies that the reconstruction error dominates the performance of the canceller. For a more accurate SI CSI, the tolerance for the delay alignment errors gradually descends if it is expected to maintain the benefit from the accurate SI CSI. For example, the cancellation is approximately unchanged for alignment errors less than 0.5% with an estimator SNR of 20 dB, whereas this range becomes less than 0.1% for an estimator SNR of 30 dB.

As a verification for proposition 3, the case for $N_t = K$ is also presented in Fig. 3. It is shown that for a large delay alignment error, $N_t = K$ benefits the canceller because at this point, the reconstruction error is the dominant and $N_t = K$ can completely removes the reconstruction error at the cost of making the canceller reduce from a ML estimator to the LS one. However, $N_t = K$ is engineering-infeasible for wide bandwidth SI signals. Proposition 3 can be only considered for a relatively-narrow SI bandwidth. This leads to the trade-off between the SI bandwidth, N_t and practical alignment errors in FD SI cancellation.

In Fig. 4, the achievable cancellation is depicted versus Doppler in Hz. The Ricean K_f−factor is a constant of 10 dB, which implies an extreme SI channel with a strong reflected path component [45]. The very case adopted for ASI cancellation is case 2 as an example, which implies the alignment error is kept negligible to achieve better cancellation. The Doppler frequency shift is up to 10 Hz, covering the Dopplers resulting from humans walking around with a signal carrier frequency of $\sim$ 2.4 GHz. Fig. 5 presents the cancellation versus Ricean K_f-factors with case 2. In Fig. 5, $\Delta T = 4$ and $\Delta T = 24$ are chosen, which respectively correspond to a short and long delay of $\sim$ 0.3 and 2 milliseconds on the order of the response time (convergence time) of current cancellers [13].

The impaired ASI cancellation is quantified in Fig. 4 and Fig. 5 with time-varying SI channels. As shown in Fig. 4 and Fig. 5, a small Doppler which usually can be neglected in conventional HD communications [46] harms the ASI cancellation severely. The impaired ASI cancellation may lead to significant lifting of nonlinearities and quantization noise in the receiver chain [24], and thus result in capacity loss for the intended signal. In this paper, the effect of larger Doppler frequency shifts on ASI cancellation is not presented specially since a Doppler frequency shift of 10 Hz with $\Delta T = 24$ already leads to significant cancellation deterioration as shown in Fig.4 and 5.

In the next section, the achievable rate gain of FD receivers with limited ADC dynamic range and linearity in the receiver chain is discussed, considering the effect of the impaired ASI cancellation over time-varying SI channels.

IV. CAPACITY OF FD TRANSCEIVERS WITH LIMITED ADC DYNAMIC RANGE AND LINEARITY

As shown in (21) in Section II, β_{INR}, which characterizes the powers of the nonlinear distortions and quantization noise, is the function of p_{rd} given in Section III. The nonlinear distortions at the receiver chain and the quantization noise induced at the ADC may be raised due to the residual SI after ASI cancellation, and thus, harm $\beta_{D,in}$. In what follows, this effect is quantized from the point of rate gain over HD receivers.

In this paper, the capacity comparison is considered over half- and full-duplex communication links (seen in Fig. 2 and 3 in [47]). The rate of an FD transceiver is written as

$$\begin{aligned} R_{FD} &= R_{FD,up} + R_{FD,dw} \\ &= 2 \times \log\left(1 + \beta_{D,in}\right), \end{aligned} \tag{41}$$

where $R_{FD,up}$ and $R_{FD,dw}$ are respectively the rate for the uplink and downlink and for simplicity, the SINRs for the reverse links are symmetric, i.e., $R_{FD,up} = R_{FD,dw}$. This paper considers β_{hf} as a constant regardless of the power of the transmit signal. It implies that the ratio of the received power of the intended signal to the thermal noise power is fixed. In this manner, β_{hf}, which depends on the path loss and transmit power of the intended signal, is separated from specific combinations of values of the path loss and the transmit power of the intended signal.

Proposition 4: For FD transceivers with limited ADC dynamic range and linearity in the receiver chain, the FD transceiver outperforms the half-duplex one if

$$\beta_{INR}^2 < \beta_{hf} + 1. \tag{42}$$

Proof: The FD transceiver outperforms the half-duplex one if

$$R_{FD} > \log\left(1 + \beta_{hf}\right). \tag{43}$$

Solving (43) yields the result in (42).

Remark 8: As indicated by (16)–(21), β_{INR} is closely related to p_{rd}, approximately, $\beta_{INR} \propto p_{rd}$. From (16), (17), and (21), β_{INR} is an increasing function of p_{rd}. Thus, the power of the residual SI signal after ASI cancellation, i.e., p_{rd}, should be upper-bounded in order to satisfy (42).

To further clarify this bound, consider the state-of-the-art wideband RF transceivers. The quantization noise is the limiting factor with the presence of SI after ASI cancellation, which means that the power of the quantization noise is much larger than the 2nd-/3rd-order nonlinear distortions [24]. Thus, (42) is approximately modified as

$$p_{rd}^2 < \frac{\beta_{hf} + 1}{\varrho^2}, \tag{44}$$

where $\varrho = 10^{\frac{\rho - 6.02b - 4.76}{10}}/\sigma^2$. This indicates the required upper-bound of p_{rd} for quantization-noise-limited FD transceivers that outperform the HD ones.

Due to the imperfect reconstruction of the SI channel and the time-varying SI channels, whose effect on the ASI cancellation has been demonstrated in Section III, the power of the residual SI after ASI cancellation may go beyond this required bound.

Considering that the power of the residual SI after ASI cancellation increases with the power of the transmit SI signal when limited ASI cancellation is achieved, the maximum allowed transmit power (MATP) of the SI, above which, the HD receiver will outperform the FD one, should also be bounded.

It is noted that β_{INR}^2 is quite nonlinear with p_{rd}. Solving (42) to determine the MATP is not feasible. In what follows, the MATP as well as the rate gain over HD receivers are quantified with imperfect reconstruction over time-varying SI channels.

TABLE 2. Parameters I: LNA Mixer and VGA.

Component	Gain (dB)	IIP2 (dBm)	IIP2 (dBm)	NF (dB)
LNA	25	43	-9	4.1
Mixer	6	42	15	4
VGA	0-69	43	14	4.1

TABLE 3. Parameters II: ADC and PAPR.

Parameter		Value
ADC	Bits	8 and 12
	Maximum Input power	5 dBm
PAPR		10 dB

A. NUMERAL RESULTS

The specified parameters for the FD receiver are given in tables II and III, which are modified from [24] for state-of-the-art receivers, and case 2 is adopted for ASI cancellation as an example.

The MATP is obtained as follows. The upper-bound for p_{rd} is first determined with (42). Then, MATP is calculated as a sum of the upper-bound, the amount of ASI cancellation given in Section III, and a gain provided by propagation-domain suppression.[3]

Fig. 6 and 7 depict the maximum allowed transmit power in time-varying SI channels with imperfect SI reconstruction and limited ADC dynamic range and linearity in the receiver chain shown in tables II and III. In both figures, β_{hf} indicates the achievable SNR for the intended signal. The ENOB of

[3]Note that in Section III, the transmit SI power is normalized to 1. The amount of ASI cancellation can be simply obtained.

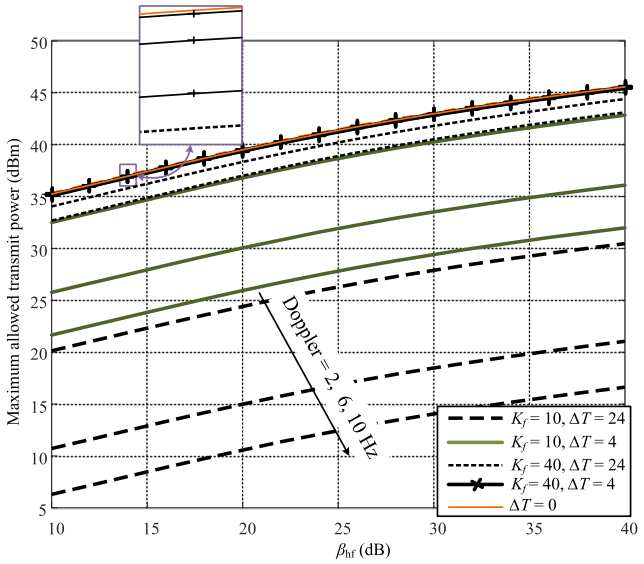

FIGURE 6. Maximum allowed transmit power in time-varying SI channel with imperfect SI reconstruction, limited receiver linearity, and limited ADC dynamic range, where the parameters are shown in tables II and III with an ADC bit of 8, the estimator SNR is 40 dB for obtaining the SI CSI, and the doppler frequency shifts are 2, 6 and 10 Hz.

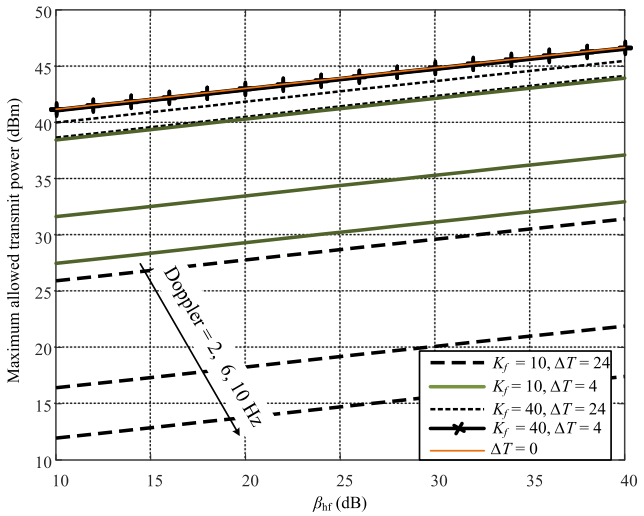

FIGURE 7. Maximum allowed transmit power in time-varying SI channel with imperfect SI reconstruction limited receiver linearity, and limited ADC dynamic range, where the parameters are shown in tables II and III with an ADC bit of 12, the estimator SNR is 40 dB for obtaining the SI CSI, and the doppler frequency shifts are 2, 6 and 10 Hz.

ADC is 8 and 12 for Fig. 6 and 7, respectively. The Reciean factors of 10 and 40 dB are chosen [45] for both figures, which respectively represents an SI channel with strong time-varying reflected-path components and with a strong line-of-sight path. Again, $\Delta T = 4$ and $\Delta T = 24$ are adopted as an example, and an estimator of 40 dB for obtaining the SI CSI is assumed. The gain provided by propagation-domain suppression is 20 dB which denotes the propagation-domain cancellation (antenna isolation) for FD radios. This value lies in the reasonable value interval of antenna isolation for both the single-antenna and the separated-antennas FD transceivers [9], [13].

As shown in Fig. 6 or 7, the MATP increases with β_{hf} in the range from 10 dB to 40 dB. A higher β_{hf} implies the intended signal has a higher power, thus, the tolerance for p_{rd} is improved, i.e., the maximum allowed transmit power can be raised. On the other hand, the MATP decreases fast as the Doppler goes from 2 Hz to 10 Hz, especially when the SI channel has a lower K_f and the ASI cancellation suffers from a larger ΔT. The sensitivity of the channel-aware ASI canceller to the doppler frequency shift limits the amount of ASI cancellation, and thus implies critical requirements on higher linearity and numbers of ADC bits or lower transmitted SI powers. In addition, comparing Fig. 6 with 7, in large β_{hf} region, increasing the ENOB of ADC contributes little to improving the MATP because the nonlinearities resulting from the residual SI signal become the dominant component (An example about the power of the nonlinearities and the quantization noise can be found in [24]).

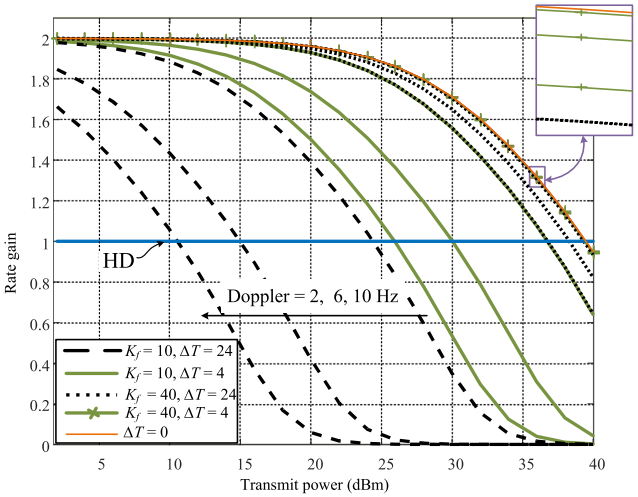

FIGURE 8. Rate gain over HD transceivers, where the parameters are shown in tables II and III with an ADC bit of 8, the estimator SNR is 40 dB for obtaining the SI CSI, and the doppler frequency shifts are 2, 6 and 10 Hz.

Fig. 8 and 9 depict the rate gains over HD receivers in time-varying SI channels with imperfect SI reconstruction, limited receiver linearity, and limited ADC dynamic range. In both figures, the transmit SI power increases from 0 dBm to 40 dBm, which is attenuated by propagation-domain suppression of 20 dB and the ASI cancellation. Then the SINR for the intended signal is obtained using (21) with $\beta_{hf} = 20\ dB$.

As shown in Fig. 8 and 9, the rate gain decreases as the transmit power grows. Increasing the transmit SI power raises the residual SI power, and thus raises the nonlinearities and quantization noise in the receiver chain, as explained in [24]. As the residual SI power goes beyond the threshold indicated by (42), the HD receiver outperforms the FD one. For FD receivers with limited ADC dynamic range and linearity, the maximum allowed transmit SI power moves left fast as the doppler frequency shift increases from 2 Hz to 10 Hz

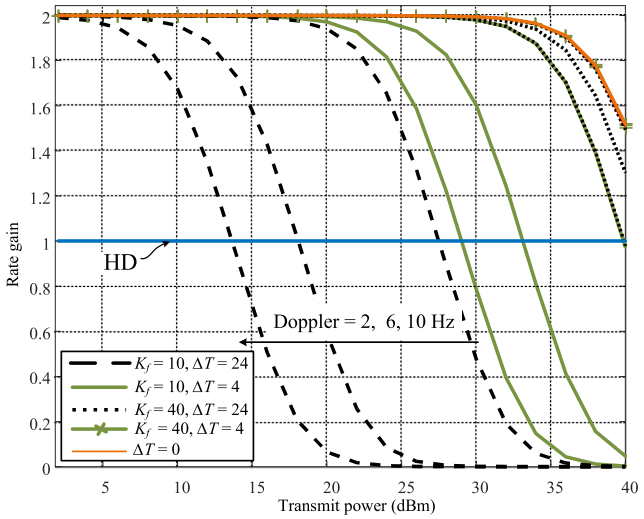

FIGURE 9. Rate gain over HD transceivers, where the parameters are shown in tables II and III with an ADC bit of 12, the estimator SNR is 40 dB for obtaining the SI CSI, and the doppler frequency shifts are 2, 6 and 10 Hz.

especially with a lower K_f and larger ΔT. Again, these results imply the sensitivity of the channel-aware ASI canceller to the doppler frequency shift which brings rate gain loss for FD receivers with limited ADC dynamic range and linearity.

V. CONCLUSION

The performance of a multi-tap canceller for full-duplex communications with imperfect self-interference CSI was analyzed in this paper. Expressions for analyzing the joint effect of imperfect SI CSI and reconstruction errors for producing the estimated response were developed for both the time-invariant and time-varying SI channels scenarios. The achievable rate of full-duplex transceivers is derived as a function of the residual SI power after the MT cancellation, dynamic range of the ADC, and the linearity of receiver chains. It was demonstrated that the tap delay alignment of the MT canceller was the critical issue in the design of the MT canceller. Deploying more taps would enlarge the effect of the imperfect CSI, and thus, harm the ASI cancellation. The sensitivity of the canceller to the doppler frequency shift reduced the amount of analog SI cancellation, and thus brought rate gain loss.

APPENDIX

The key idea is to make $\Re$ and $\Omega\Omega^H$ respectively a diagonal matrix. Matrix $\Omega\Re^{-1}\Omega^H$ becomes an identity matrix if

$$\begin{cases} \Re_{ij} = 0, & i \neq j \\ \left(\Omega\Omega^H\right)_{ij} = 0, & i \neq j \\ \left(\Omega\Omega^H\right)_{ij}/\Re_{ij} = 1, & i = j. \end{cases} \tag{45}$$

The entries of $\Re$ except the diagonal ones can be written as

$$\Re_{ij} = e^{j\Delta_w(\tau_i-\tau_j)}\frac{1-e^{j\Delta_w K(\tau_i-\tau_j)}}{1-e^{j\Delta_w(\tau_i-\tau_j)}},\ i \neq j. \tag{46}$$

For a uniform interval of tap delay, i.e., $\Delta t = \tau_{i+1} - \tau_i$, the entries of $\Re$ given in (46) can be rewritten as

$$\Re_{ij} = \begin{cases} e^{j\Delta_w(j-i)\Delta t}\dfrac{1-e^{j\Delta_w K(j-i)\Delta t}}{1-e^{j\Delta_w(j-i)\Delta t}}, & j < i \\ e^{j\Delta_w(i-j)\Delta t}\dfrac{1-e^{j\Delta_w K(i-j)\Delta t}}{1-e^{j\Delta_w(i-j)\Delta t}}, & j > i \end{cases}. \tag{47}$$

Matrix $\Omega\Omega^H$ is calculated as (48) shown at the bottom of this page. The entries of $\Omega\Omega^H$ except the diagonal ones can be written as

$$\left(\Omega\Omega^H\right)_{ij} = \begin{cases} e^{j\Delta_w(j-i)\tau_0}\dfrac{1-e^{j\Delta_w N_t(j-i)\Delta t}}{1-e^{j\Delta_w(j-i)\Delta t}}, & j < i \\ e^{j\Delta_w(i-j)\tau_0}\dfrac{1-e^{j\Delta_w N_t(i-j)\Delta t}}{1-e^{j\Delta_w(i-j)\Delta t}}, & j > i, \end{cases} \tag{49}$$

with $\Delta t = \tau_{i+1} - \tau_i$. By substituting (47) and (49) into (45), it follows

$$\begin{cases} \Delta_w K\xi\Delta t = 2p\pi \\ \Delta_w\xi\Delta t \neq 2q\pi \\ \Delta_w N_t\lambda\Delta t = 2u\pi \\ \Delta_w\lambda\Delta t \neq 2v\pi \\ N_t = K, \end{cases} \tag{50}$$

where $p, q, u, v \in Z$, $\xi = \pm 1, \pm 2, \ldots \pm K - 1$, and $\lambda = \pm 1, \pm 2, \ldots \pm N_t - 1$. By solving (50), it leads to

$$N_t = K \tag{51}$$

and

$$\Delta t = \frac{2p\pi}{\Delta_w K} = \frac{p}{B}, \tag{52}$$

where p should be chosen such that the inequalities in (50) hold. In particular, $p = 1$ is adopted, and thus it follows $\Delta t = 1/B$. ■

$$\Omega\Omega^H = \begin{bmatrix} N_t & e^{j\Delta_w\tau_0}\dfrac{1-e^{j\Delta_w N_t\Delta t}}{1-e^{j\Delta_w\Delta t}} & \cdots & e^{j(K-1)\Delta_w\tau_0}\dfrac{1-e^{j(K-1)\Delta_w N_t\Delta t}}{1-e^{j(K-1)\Delta_w\Delta t}} \\ e^{-j\Delta_w\tau_0}\dfrac{1-e^{-j\Delta_w N_t\Delta t}}{1-e^{-j\Delta_w\Delta t}} & N_t & \cdots & e^{j(K-2)\Delta_w\tau_0}\dfrac{1-e^{j(K-2)\Delta_w N_t\Delta t}}{1-e^{j(K-2)\Delta_w\Delta t}} \\ \vdots & \vdots & \ddots & \vdots \\ e^{-j(K-1)\Delta_w\tau_0}\dfrac{1-e^{-j(K-1)\Delta_w N_t\Delta t}}{1-e^{-j(K-1)\Delta_w\Delta t}} & e^{-j(K-2)\Delta_w\tau_0}\dfrac{1-e^{-j(K-2)\Delta_w N_t\Delta t}}{1-e^{-j(K-2)\Delta_w\Delta t}} & \cdots & N_t \end{bmatrix} \tag{48}$$

VI. ACKNOWLEDGMENT

This paper was presented at the IEEE GLOBECOM Workshop on Full Duplex Wireless Communications 2016.

REFERENCES

[1] A. A. Zaidi *et al.*, "Waveform and numerology to support 5G services and requirements," *IEEE Commun. Mag.*, vol. 54, no. 11, pp. 90–98, Nov. 2016.

[2] C.-X. Wang *et al.*, "Cellular architecture and key technologies for 5G wireless communication networks," *IEEE Commun. Mag.*, vol. 52, no. 2, pp. 122–130, Feb. 2014.

[3] A. Sabharwal, P. Schniter, D. Guo, D. W. Bliss, S. Rangarajan, and R. Wichman, "In-band full-duplex wireless: Challenges and opportunities," *IEEE J. Sel. Areas Commun.*, vol. 32, no. 9, pp. 1637–1652, Sep. 2014.

[4] X. Wang, H. Huang, and T. Hwang, "On the capacity gain from full duplex communications in a large scale wireless network," *IEEE Trans. Mobile Comput.*, vol. 15, no. 9, pp. 2290–2303, Sep. 2016.

[5] D. Kim, H. Lee, and D. Hong, "A survey of in-band full-duplex transmission: From the perspective of PHY and MAC layers," *IEEE Commun. Surveys Tuts.*, vol. 17, no. 4, pp. 2017–2046, 4th Quart., 2015.

[6] D. Kim, S. Park, H. Ju, and D. Hong, "Transmission capacity of full-duplex-based two-way ad hoc networks with ARQ protocol," *IEEE Trans. Veh. Technol.*, vol. 63, no. 7, pp. 3167–3183, Sep. 2014.

[7] F. Zhu, F. Gao, T. Zhang, K. Sun, and M. Yao, "Physical-layer security for full duplex communications with self-interference mitigation," *IEEE Trans. Wireless Commun.*, vol. 15, no. 1, pp. 329–340, Jan. 2016.

[8] G. Zheng, I. Krikidis, J. Li, A. P. Petropulu, and B. Ottersten, "Improving physical layer secrecy using full-duplex jamming receivers," *IEEE Trans. Signal Process.*, vol. 61, no. 20, pp. 4962–4974, Oct. 2013.

[9] E. Everett, A. Sahai, and A. Sabharwal, "Passive self-interference suppression for full-duplex infrastructure nodes," *IEEE Trans. Wireless Commun.*, vol. 13, no. 2, pp. 680–694, Jan. 2014.

[10] E. Aryafar, M. Khojastepour, K. Sundaresan, S. Rangarajan, and M. Chiang, "MIDU: Enabling MIMO full duplex," in *Proc. ACM MobiCom*, 2012, pp. 257–268.

[11] J. I. Choi, M. Jain, K. Srinivasan, P. Levis, and S. Katti, "Achieving single channel full duplex wireless communications," in *Proc. ACM MobiCom*, 2010, pp. 1–12.

[12] Y. Hua, P. Liang, Y. Ma, A. C. Cirik, and Q. Gao, "A method for broadband full-duplex MIMO radio," *IEEE Signal Process. Lett.*, vol. 19, no. 12, pp. 793–796, Dec. 2012.

[13] D. Bharadia, E. McMilin, and S. Katti, "Full duplex radios," in *Proc. ACM SIGCOM*, 2013, pp. 375–386.

[14] L. Laughlin, M. A. Beach, K. A. Morris, and J. L. Haine, "Optimum single antenna full duplex using hybrid junctions," *IEEE J. Sel. Areas Commun.*, vol. 32, no. 9, pp. 1653–1661, Sep. 2014.

[15] B. Debaillie *et al.*, "Analog/RF solutions enabling compact full-duplex radios," *IEEE J. Sel. Areas Commun.*, vol. 32, no. 9, pp. 1662–1673, Sep. 2014.

[16] D. Liu, S. Shao, Y. Shen, Q. Liang, and Z. Lu, "Analysis of analog self-interference cancellation with imperfect channel state information for full-duplex radios," in *Proc. IEEE GLOBECOM*, Dec. 2016, pp. 1–6.

[17] A. Masmoudi and T. Le-Ngoc, "Channel estimation and self-interference cancelation in full-duplex communication systems," *IEEE Trans. Veh. Technol.*, vol. 66, no. 1, pp. 321–334, Jan. 2017, doi: 10.1109/TVT.2016.2540538

[18] K. E. Kolodziej, J. G. McMichael, and B. T. Perry, "Multitap RF canceller for in-band full-duplex wireless communications," *IEEE Trans. Wireless Commun.*, vol. 15, no. 6, pp. 4321–4334, Jun. 2016.

[19] M. Duarte and A. Sabharwal, "Full-duplex wireless communications using off-the-shelf radios: Feasibility and first results," in *Proc. Conf. Rec. 44th Asilomar Conf. Signals, Syst. Comput.*, Nov. 2010, pp. 1558–1562.

[20] Y.-S. Choi and H. Shirani-Mehr, "Simultaneous transmission and reception: Algorithm, design and system level performance," *IEEE Trans. Wireless Commun.*, vol. 12, no. 12, pp. 5992–6010, Dec. 2013.

[21] Z. Zhang, Y. Shen, S. Shao, W. Pan, and Y. Tang, "Full duplex 2×2 MIMO radios," in *Proc. 6th Int. Conf. Wireless Commun. Signal Process.(WCSP)*, Oct. 2014, pp. 1–6.

[22] L. Sun, Y. Li, Y. Zhao, L. Huang, and Z. Gao, "Optimized adaptive algorithm of digital self-interference cancellation based on improved variable step," in *Proc. IEEE 9th Int. Conf. Anti-Counterfeiting, Secur., Identificat. (ASID)*, Xiamen, China, Sep. 2015, pp. 176–179.

[23] J. G. McMichael and K. E. Kolodziej, "Optimal tuning of analog self-interference cancellers for full-duplex wireless communication," in *Proc. 50th Annu. Allerton Conf. Commun., Control, Comput. (Allerton)*, Oct. 2012, pp. 246–251.

[24] D. Korpi, T. Riihonen, V. Syrjala, L. Anttila, M. Valkama, and R. Wichman, "Full-duplex transceiver system calculations: Analysis of adc and linearity challenges," *IEEE Trans. Wireless Commun.*, vol. 13, no. 7, pp. 3821–3836, Jul. 2014.

[25] L. M. O. R. T. Samara; Mokhtar; Ozdemir; Hamila; Khattab, "Residual loop-back self-interference analysis for full-duplex OFDM transceivers under phase noise and I/Q imbalance," *IEEE Commun. Lett.*, vol. 21, no. 2, pp. 314–317, Feb. 2017, doi: 10.1109/LCOMM.2016.2620431.

[26] A. Sahai, G. Patel, C. Dick, and A. Sabharwal, "On the impact of phase noise on active cancelation in wireless full-duplex," *IEEE Trans. Veh. Technol.*, vol. 62, no. 9, pp. 4494–4510, Nov. 2013.

[27] V. Syrjala, M. Valkama, L. Anttila, T. Riihonen, and D. Korpi, "Analysis of oscillator phase-noise effects on self-interference cancellation in full-duplex OFDM radio transceivers," *IEEE Trans. Wireless Commun.*, vol. 13, no. 6, pp. 2977–2990, Jun. 2014.

[28] D. Korpi *et al.*, "Full-duplex mobile device: Pushing the limits," *IEEE Commun. Mag.*, vol. 54, no. 9, pp. 80–87, Sep. 2016.

[29] X. Zhang, W. Cheng, and H. Zhang, "Full-duplex transmission in PHY and MAC layers for 5G mobile wireless networks," *IEEE Wireless Commun.*, vol. 22, no. 5, pp. 112–121, Oct. 2015.

[30] H. Lu, S. Shao, K. Deng, and Y. Tang, "Self-mixed self-interference analog cancellation in full-duplex communications," *Sci. China Inf. Sci.*, vol. 59, no. 4, pp. 3737–3741, Apr. 2016.

[31] Y. Liu, X. Quan, W. Pan, S. Shao, and Y. Tang, "Nonlinear distortion suppression for active analog self-interference cancellers in full duplex wireless communication," in *Proc. IEEE Globecom*, Austin, TX, USA, Dec. 2014, pp. 948–953.

[32] Q. Gu, *RF System Design of Transceivers for Wireless Communications*. Secaucus, NJ, USA: Springer-Verlag, 2006.

[33] M. C. Jeruchim, P. Balaban, and K. S. Shanmugan, *Simulation of Communication Systems*, 2nd ed. New York, NY, USA: Kluwer, 2000.

[34] D. Tse and P. Viswanath, *Fundamentals of Wireless Communication*, Cambridge, U.K.: Cambridge Univ. Press, 2005.

[35] Y. Li, "Pilot-symbol-aided channel estimation for OFDM in wireless systems," *IEEE Trans. Veh. Technol.*, vol. 49, no. 4, pp. 1207–1215, Jul. 2000.

[36] H. Suzuki, T. V. A. Tran, I. B. Collings, G. Daniels, and M. Hedley, "Transmitter noise effect on the performance of a MIMO-OFDM hardware implementation achieving improved coverage," *IEEE J. Sel. Areas Commun.*, vol. 26, no. 6, pp. 867–876, Aug. 2008.

[37] D. Liu, W. Ma, S. Shao, Y. Shen, and Y. Tang, "Performance analysis of TDD reciprocity calibration for massive MU-MIMO systems with ZF beamforming," *IEEE Commun. Lett.*, vol. 20, no. 1, pp. 113–116, Jan. 2015.

[38] M. Morelli and U. Mengali, "A comparison of pilot-aided channel estimation methods for OFDM systems," *IEEE Trans. Signal Process.*, vol. 49, no. 12, pp. 3065–3073, Dec. 2001.

[39] S. Haykin, *Adaptive Filter Theory*, 4th ed. Upper Saddle River, NJ, USA: Prentice-Hall, 2001.

[40] M. Duarte, C. Dick, and A. Sabharwal, "Experiment driven characterization of full-duplex wireless communications," *IEEE Trans. Wireless. Commun.*, vol. 11, no. 12, pp. 4296–4307, Dec. 2012.

[41] P. Tan and N. C. Beaulieu, "Effect of channel estimation error on bit error probability in OFDM systems over rayleigh and ricean fading channels," *IEEE Trans. Commun.*, vol. 56, no. 4, pp. 675–685, Apr. 2008.

[42] M. D. Yacoub, *Foundations of Mobile Radio Engineering*. Boca Raton, FL, USA: CRC Press, 1993.

[43] S. B. Bulumulla, S. A. Kassam, and S. S. Venkatesh, "A systematic approach to detecting OFDM signals in a fading channel," *IEEE Trans. Commun.*, vol. 48, no. 5, pp. 725–728, May 2000.

[44] X. Wu, Y. Shen, and Y. Tang, "The power delay profile of the single-antenna full-duplex self-interference channel in indoor environments at 2.6 GHz," *IEEE Antennas Wireless Propag. Lett.*, vol. 13, pp. 1561–1564, Aug. 2014.

[45] M. E. Knox, "Single antenna full duplex communications using a common carrier," in *Proc. IEEE 13th Annu. Wireless Microw. Technol. Conf. (WAMICON)*, Apr. 2012, pp. 1–6.

[46] S. Y. Leong, J. Wu, C. Xiao, and J. C. Olivier, "Fast time-varying dispersive channel estimation and equalization for an 8-PSK cellular system," *IEEE Trans. Veh. Technol.*, vol. 55, no. 5, pp. 1493–1502, Sep. 2006.
[47] W. Li, J. Lilleberg, and K. Rikkinen, "On rate region analysis of half- and full-duplex OFDM communication links," *IEEE J. Sel. Areas Commun.*, vol. 32, no. 9, pp. 1688–1698, Sep. 2014.

DONGLIN LIU received the B.E. degree in communication engineering from the University of Electronic Science and Technology of China, Chengdu, China, in 2013, where he is currently pursuing the Ph.D. degree in information and communication engineering with the National Key Laboratory of Science and Technology on Communications.

YING SHEN received the B.E. and Ph.D. degrees in communications and information systems from the University of Electronic Science and Technology of China, Chengdu, China, in 2002 and 2009, respectively. His research interests include MIMO and full-duplex communications.

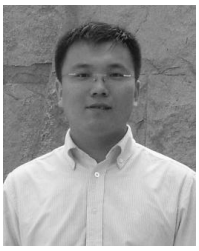

SHIHAI SHAO (S'05–M'10) received the B.E. and Ph.D. degrees in communication and information systems from the University of Electronic Science and Technology of China (UESTC), Chengdu, China, in 2003 and 2008, respectively. Since 2015, he has been a Professor with the National Key Laboratory of Science and Technology on Communications, UESTC. His current research interests include the design, modeling, and the analysis of full-duplex transceivers, MIMO detection, and all-digital transceivers.

YOUXI TANG received the B.E. degree in radar engineering from the College of PLA Ordnance, Shijiazhuang, China, in 1985, and the M.S. and Ph.D. degrees in communications and information systems from the University of Electronic Science and Technology of China, Chengdu, China, in 1993 and 1997, respectively. From 1998 to 2000, he was a Program Manager with Huawei Technologies Co., Ltd., Shanghai, China, where he was involved in IS-95 mobile communications and third-generation mobile communications. Since 2004, he has been a Professor with the National Key Laboratory of Science and Technology on Communications, University of Electronic Science and Technology of China. He has authored or co-authored several books. The latest one is *No Division Duplex-Full Duplex Principles and Applications* (Science Press). His main research interests include full duplex and MIMO, with emphasis on signal processing in communications.

YI GONG (S'99–M'03–SM'07) received the Ph.D. degree in electrical engineering from The Hong Kong University of Science and Technology, Hong Kong, in 2002. He joined the Hong Kong Applied Science and Technology Research Institute, Hong Kong, as a member of the Professional Staff. He was with Nanyang Technological University, Singapore, where he still has active collaborations. He is currently a Professor with the Southern University of Science and Technology, Shenzhen, China. His research interests include multi-antenna and cooperative communications, cognitive and full-duplex radio, cross-layer design, and physical layer security for wireless systems. Since 2006, he has been serving on the Editorial Board of the IEEE TRANSACTIONS ON WIRELESS COMMUNICATIONS and the IEEE TRANSACTIONS ON VEHICULAR TECHNOLOGY.